Building Effects of Irregular Site Condition on Seismic Response of Nuclear Power Plant

M. Watabe

University of Tokyo Metropolitan, Architectural Dept., 2-1-1, Fukazawa, Setagaya-ku, Tokyo 158, Japan

H. Yamanouchi, I. Ohkawa

Ministry of Construction, Building Research Institute, Tachihara-1, Oho-cho, Tsukuba-gun, Ibaraki, Japan

O. Chiba, M. Tohdo

Toda Construction Co., Ltd., Structural Engineering Dept., 7-1, Kyobashi 1-chome, Chuo-ku, Tokyo 104, Japan

ABSTRACT

The effects of topographical irregularities in the local sites to the seismic responses of a nuclear reactor building have been investigated. First of all, the surface ground motion is obtained by the method of boundary integration equations utilizing the Green's functions. Next, the seismic response analyses with various parameters on site condition have been carried out. Consequently, it has been found that in the local site having the ground surface different in level, the responses on the terrace are rather affected by the slope, but the effect of slope on the low ground is small. In the site with inclined interface between two layers, when the inclination is large, the influence by that cannot be ignored.

1. Introduction

It is generally observed in the local site that the ground surface differrent in level such as terrace and low ground exists, or the configuration of the layer of local soil deposit is not horizontal. In Japan the severe damage during various earthquakes, e.g. Tokachi-oki earthquake of May 16, 1968 and Miyagi-ken-oki earthquake of June 12, 1978 were often caused at the sites with topographical irregularities mentioned above. One of the factors influencing the above phenomena seems to be the complex reflection, refraction and diffraction of the seismic wave during propagation by the sudden change of transmitted soil medium. Therefore, it will be necessary to investigate the influence of topographically irregular site condition to earthquake response of nuclear power plants in the seismic design.

From the above descrived point of view, this paper presents the results of seismic response analysis of a nuclear reactor building on the local site with various topographical irregularities. As is shown in Fig.1, the effects to response of buildings due to the three kinds of site conditions are investigated, depending on the topographic irregularities;

1) Condition-L : the irregular configuration of ground surface different in level
2) Condition-D : the two-layered soil deposit with inclined interface
3) Condition-C : the irregular condition of site combined with Condition-L and D

2. Mathematical model to obtain the surface ground motion

In order to obtain the input motion to buildings due to incident seismic wave, the Green's function method is used. The total wave motions (displacement u and surface traction t) at a point (a) in the field are expressed by the sum of motions (u_{in} , t_{in}) in semi-infinite medium without irregularity subjected to incident wave and the scattering wave (u_{s} , t_{s}), therefore the equations can be obtained as follows:

$$u^{r}(a^{r}) = u^{r}_{in}(a^{r}) + u^{r}_{s}(a^{r})$$
$$t^{r}(a^{r}) = t^{r}_{in}(a^{r}) + t^{r}_{s}(a^{r}) \qquad (1)$$

where r denotes the region-1 or region-2 illustrated in Fig.2.

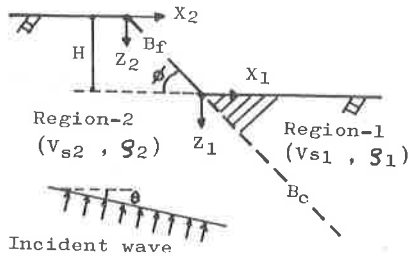

Fig.2 Analytical model of a site with topographical irregularity

The wave scattered by the irregular boundary can be given by:

$$u^{r}_{s}(a^{r}) = \int_{B} g(a^{r}, b^{r}_{o})\cdot p^{r}(b^{r}_{o})\cdot dB^{r}$$
$$t^{r}_{s}(a^{r}) = \int_{B} h(a^{r}, b^{r}_{o})\cdot p^{r}(b^{r}_{o})\cdot dB^{r} \qquad (2)$$

in which B^{r} denotes the boundary, b^{r}_{o} is a point on B^{r}, and $p^{r}(b^{r}_{o})$ is the unknown potentials distributed on B^{r}. Then g(a,b) and h(a,b) are the Green's functions.

Now consider the anti-plane problem subjected to incident SH-wave. In this case, the motions u_{in} and the Green's function g become

$$u_{in}(a)=E\cdot\exp(ikx\cdot\sin\theta)\cdot\{\exp(-ikz\cdot\cos\theta)+\exp(ikz\cdot\sin\theta)\} \quad , \ i=\sqrt{-1} \qquad (3)$$
$$g(a,b)=\{H^{(1)}_{0}(kd)+H^{(1)}_{0}(kd')\}\cdot i/(4\mu) \quad , \ d \text{ and } d'=\sqrt{(x-x_b)^2+(z\mp z_b)^2} \qquad (4)$$

in which θ is an angle of incidence, k is a wave number (=ω/Vs) and $H^{(1)}_{0}$ is the Hankel's function of the first kind of order zero. Since the tractions obtained in Eqs.(3) and (4) are zero at z=0, it is not necessary to satisfy the free surface condition in solving the equations.

As a → b in Eq.(1), this equation becomes the boundary integration equations. In this paper, because of the difficulty of solving the equations the computations are carried out by discretizing the boundary under the assumptions in which the tractions and potentials are constant in each boundary element and the displacement is evaluated at the center of an element. Considering the boundary conditions of free surface Bf and the continuity of traction and displacement on Bc, the boundary equations can be written in the matrix form;

$$\begin{bmatrix} \underline{G}^1 & -\underline{G}^2_{cc} & -\underline{G}^2_{cf} \\ \underline{H}^1 & \underline{H}^2_{cc} & \underline{H}^2_{cf} \\ \underline{0} & \underline{H}^2_{fc} & \underline{H}^2_{ff} \end{bmatrix} \cdot \begin{Bmatrix} P^1 \\ P^2_c \\ P^2_f \end{Bmatrix} = \begin{Bmatrix} -u^1_{in} + u^2_{in,c} \\ -T^1_{in} - T^2_{in,c} \\ -T^2_{in,f} \end{Bmatrix} \qquad (5)$$

Where superscripts 1 and 2 show region numbers and a subscript c or f means that its submatrix or vector is related to Bc or Bf shown in Fig.2. In Eq.(5) the elements of matrices $\underline{G}$ and $\underline{H}$ are expressed by

$$G_{ij} = \left[\int_{\Delta B_j} g(b_i, b_{oj})\cdot d\Delta B_j\right] / \Delta B_j$$
$$H_{ij} = \alpha_{ij} + \left[\int_{\Delta B_j} h(b_i, b_{oj})\cdot d\Delta B_j\right] \Delta B_i/\Delta B_j \qquad (6)$$

in which ΔB indicates the area of a discrete element and α_{ij} is the coefficient to express a singular point within integration of equation (6).

Solving Eq.(5), the displacement at a point in the field can be calculated by substitution of the potentials into Eq.(1).

3. Numerical examples of surface ground motions

Based on the method described above, the numerical examples of amplifications of surface ground motions to an amplitude of incident harmonic motion are presented in this chapter, depending on the various cases of topography. The vertical incidence ($\theta=0^\circ$) is assumed for the wave propagation in any case.

Fig.3 presents the amplification patterns for the Condition-L shown in Fig.1(a) with the parameters of slope angles ϕ of 20°, 30°, 45° and 60°. In the figure the horizontal axis indicates the dimensionless coordinate x/H and the variable η is dimensionless frequency fH/V_S. It is noted here that when the surface is flat, the amplification becomes the constant value of 2. From the results it is seen that the variations of amplifications in terms of η on the terrace are larger than those on the low ground. It will be explained by the fact that the wave propagation reflected by slope mainly directs toward the left hand side in Fig.1. This phenomenon leads to the fact that ϕ being close to 45°, the variation of amplification on the terrace becomes much larger.

The results for Condition-D in Fig.1(b) are plotted in Fig.4 with the inclination of 20° or 30° of interface. In this analysis, the ratio V_{S2}/V_{S1} is two. In Fig.4 the horizontal axis shows dimensionless frequency k·x in which k is the wave number of surface layer. Then the dotted line shows the amplification in the case of flat surface layer having the depth between surface and base layer at a point x. These results indicate that as the inclination ϕ becomes large, the amplification and the predominant period increasingly vary with the freqnency k and the coordinate x in comparison with the amplification of soil deposit assumed flat layer.

The amplifications for Condition-C in Fig.1(c) are presented in Fig.5, in which the variable η is dimensionless frequency fH/V_{S1} and V_{S2}/V_{S1} is 2. Taking twice of η in Fig.3, the results on terrace in Fig.5 could be compared with those in Fig.3, and the results on low ground in Fig.5 with those in Fig.4 when kx is divided by $2\pi x/H$. Under the consideration of above fact it is seen that the amplification characteristics on the terrace are hardly affected by the existence of softer surface layer and those on low ground only slightly by the slope.

4. Seismic response analyses of a BWR reactor building

Using the previous results, the seismic response analyses of a BWR building located on the topographically irregular site as shown in Fig.1 are carried out, with the random vibration theory.[1] A BWR building is modelled into a lumped-mass model as illustrated in Fig.6, having the soil-foundation interaction effect. For the shear wave velocity of soil deposit, it is assumed that V_S in Fig.1(a) or V_{S2} in Fig.1(b) and 1(c) is 1200m/sec and V_{S1} in Fig.1(b) and 1(c) is 600m/sec. The incident wave defined on base rock is characterized by power spectra as

$$S(\omega) = \left|\omega^2/(\omega^2+\alpha^2)\cdot\exp(-q\omega)\right|^2\cdot S_0 \qquad (7)$$

with the duration time of 9.33sec for stationary wave. In Eq.(7) the predominant period Tp of spectra is 0.3sec, $(\alpha Tp/2\pi)^2$ is 0.3 and S_0 is $232.5\,gal^2\cdot sec$. The solid line in Fig.7 shows the response spectra of doubled incident wave in comparison with the Ohsaki spectra plotted in dotted line, corresponding to S1 earthquake reduced to 81% because of harder rock.[2]

The impedance functions solved in horizontally two-layered soil deposit are used in this paper, since it is difficult to solve the 3-dimensional impedance problem in the condition shown in Fig.1. Fig.8 shows the examples of impedance functions. Then the input motion is represented by the surface ground motion at the center of foundation obtained without the structure.

Fig.9 shows the floor response spectra at base mat and the shear force of a structure located at x1=50m and x2=-100m, having the parameter of the angle ϕ of slope with the height H of 100m in Condition-L. The results indicate that the variations of building response on the terrace become large with the increase of angle ϕ of slope, on the other hand, a structure on the low ground is hardly influenced by the slope.

Fig.10 shows the results for the building at the depth of 40m and 80m of surface layer just below the structure, in terms of inclination ϕ of the interface in Condition-D. Thus, though the responses in $\phi=10^\circ$ is almost same as those in flat layer ($\phi= 0^\circ$), the responses in $\phi\geq20^\circ$ become rather different from those in $\phi=10^\circ$.

For the Condition-C, the floor response spectra of a structure at x1=50m and 100m are shown in Fig.11 with respect to the height H in the case of slope angle $\phi=20^\circ$. The level difference hardly influences the responses, therefore, only the problem of inclination of interface between layers might be taken into account in the analyses.

5. Conclusions

The parametric studies on the effects of irregular topographical conditions in Fig.1 to seismic responses of a BWR building have been made. The conclusions are summarized as follows:

1) At the local site in the ground surfaces different in level, the responses of a structure on the terrace are affected by the topographical irregularity with slope angle greater than 20°. On the other hand, such topography hardly influences responses of a structure on the low-ground.
2) At the local site with the inclined interface between two layers, when the inclination is over 10°, the effect of inclination should be considered, otherwise the analytical results may be erroneous.

REFERENCES

1) Watabe, M., Chiba, O. and Tohdo, M., 1979, "Generation of simulated three-dimensional earthquake ground motions", 5th SMiRT, K1/2

2) Tohdo, M., 1982, "Dynamic properties of embedded foundations", 6th Japan Earthquake Engineering Sympsium, No. 220

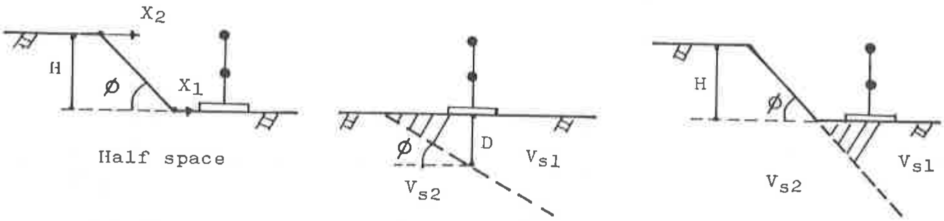

a) Condition-L b) Condition-D c) Condition-C

Fig.1 Three kinds of irregular site condition to analyse

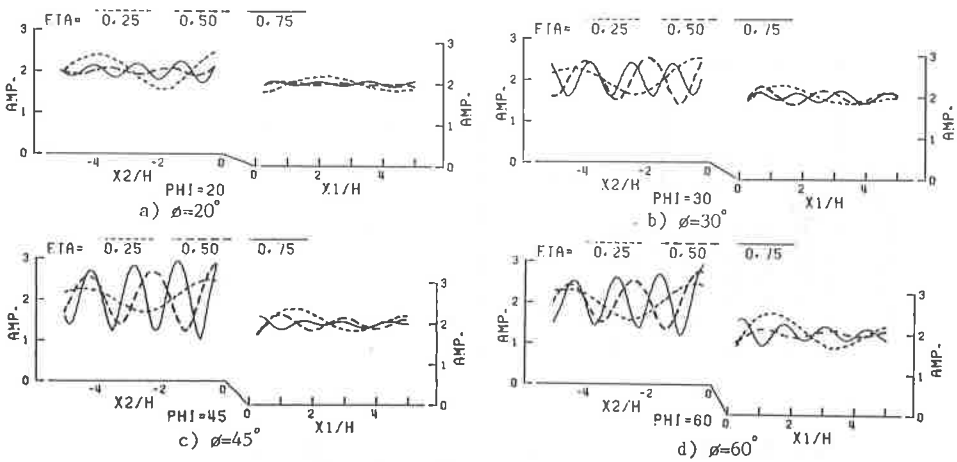

Fig.3 Amplification patterns in Condition-L

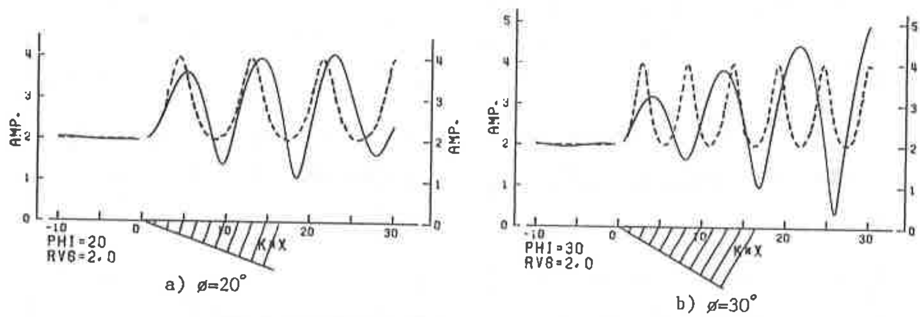

Fig.4 Amplification patterns in Condition-D

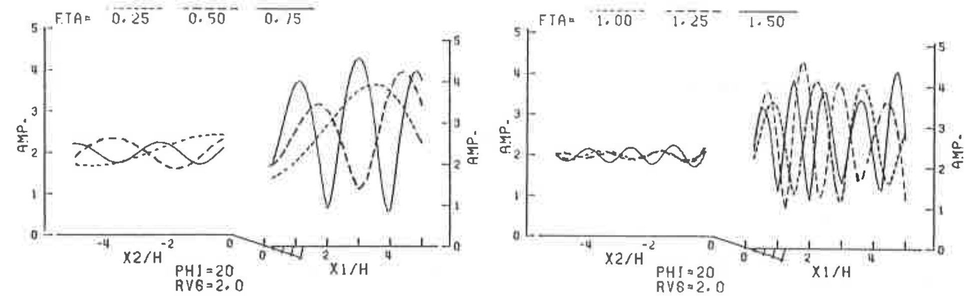

Fig.5 Amplification patterns in Condition-C

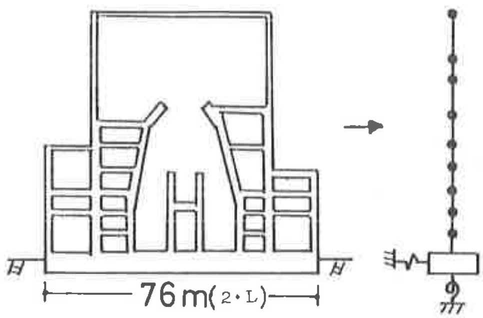

Fig.6 Modelling of a BWR building

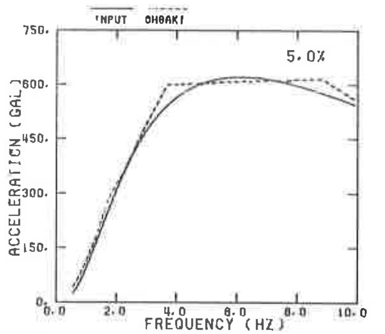

Fig.7 Comparison between response spectra of doubled incident wave and Japanese design spectra

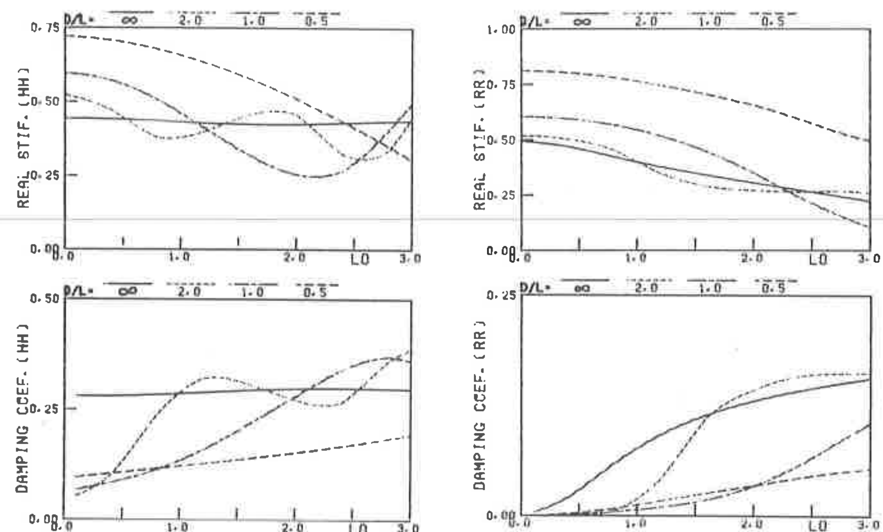

a) swaying b) rocking

Fig.8 Impedance functions of foundations on a horizontally two-layered soil

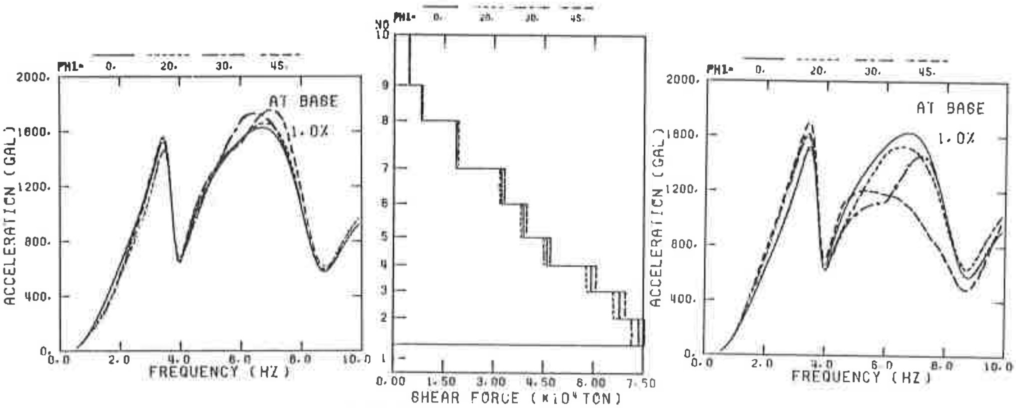

a) X1=50m

b) X2=-100m

Fig.9 Results of seismic response analyses in terms of ø of Condition-L

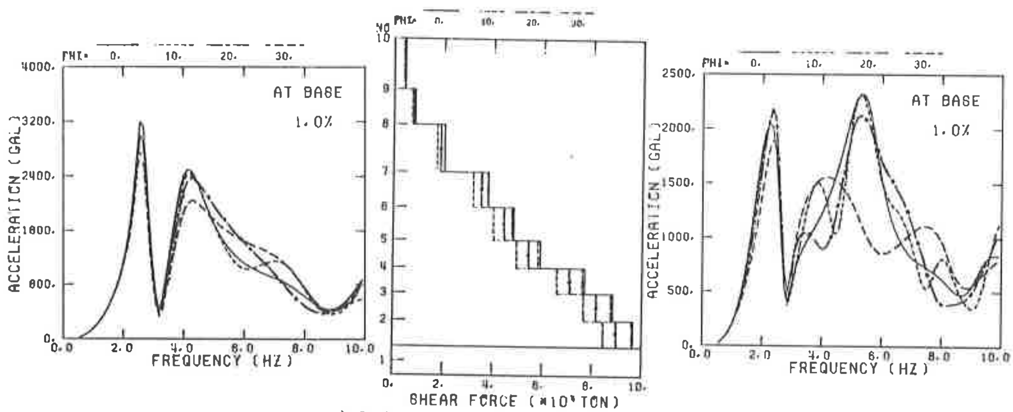

a) D=40m

b) D=80m

Fig.10 Results of seismic response analyses in terms of ø of Condition-D

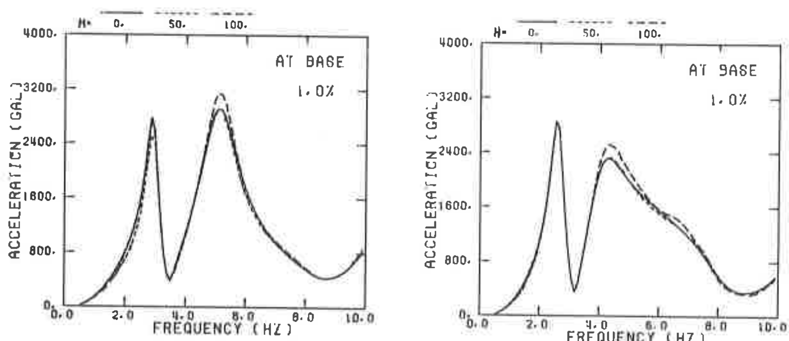

a) X1=50m

b) x1=100m

Fig.11 Results of seismic response analyses in terms of H of Condition-C